Self-referenced Doppler optical coherence tomography

Siavash Yazdanfar and Joseph A. Izatt

Department of Biomedical Engineering, Duke University, Durham, North Carolina 27708

Received June 25, 2002

Doppler optical coherence tomography (DOCT) allows simultaneous micrometer-scale resolution cross-sectional imaging of tissue structure and blood flow. We demonstrate a fiber-optic polarization-diversity-based differential phase contrast DOCT system as a method to perform self-referenced velocimetry in highly scattering media. Using this strategy, we reduced common-mode interferometer noise to <1 Hz and improved Doppler estimates in a scattering flow phantom by a factor of 5. © 2002 Optical Society of America

OCIS codes: 170.4500, 170.3340, 170.3890.

Optical coherence tomography[1] (OCT) is a noninvasive cross-sectional imaging modality capable of delineating tissue microstructure with micrometer-scale resolution in three dimensions. Phase-sensitive demodulation[2] and Hilbert transformation[3] of the interferometric OCT detector signal have been used to extract depth-resolved phase information to measure blood flow with picoliter volumetric resolution in living tissues. This functional extension of OCT, called Doppler optical coherence tomography (DOCT),[2–6] was recently demonstrated for velocimetry in human retina[5] and skin.[3]

The practical frequency (and thus velocity) precision in DOCT is often limited by sources of frequency ambiguity such as speckle modulation of the backscatter spectrum,[4] Brownian motion,[7] or interferometer noise.[8] Whereas the first two are spectroscopic features that one can exploit to determine statistical properties of the sample, interferometer jitter can corrupt spectroscopic and phase measurements. Measuring the sample-arm phase relative to a second beam (e.g., an orthogonal polarization state[9,10] or a second wavelength[11]) allows accurate phase detection that is insensitive to extraneous interferometer phase noise. This method of differential phase contrast has been used for nanometer-scale optical ranging,[12] detection of cell volume fluctuations,[13] and absolute refractive-index measurement.[14] In this Letter we demonstrate a fiber-optic polarization-diversity-based differential phase contrast OCT system as a method to perform self-referenced Doppler velocimetry in highly scattering media.

A schematic of the self-referenced DOCT Michelson interferometer is shown in Fig. 1. Collimated sample-arm light was separated into orthogonal polarization states with a Wollaston prism, resulting in an angular separation ($\alpha = 0.5°$). An objective lens located a focal length $f = 100.00$ mm from the prism made parallel and focused the two beams, resulting in a theoretical lateral focal separation $\Delta x = f\alpha = 873$ μm (measured, 863 μm) on the sample. Polarization paddles in the sample arm were used to balance the optical power in the two incident polarization states. Reference-arm scanning was performed with a retroreflecting mirror mounted on a galvanometer scanning at 33.8 mm/s. A polarizing beam splitter separated the returning sample and reference beams into orthogonal polarization states, each incident on independent photodetectors. We adjusted polarization paddles in the fiber leading to the detector to match the polarization states that were incident on the sample and to minimize cross talk between the two channels. To minimize electronic phase noise, two phase-locked lock-in amplifiers performed coherent (phase-sensitive) demodulation of the photodetector output at the nominal Doppler frequency ($f_r = 81.8$ kHz) induced by reference scanning. Demodulation prior to data acquisition shifted the DOCT spectrum down to baseband while preserving both the amplitude and the phase of the detector signal. Therefore demodulation had the advantage of reducing the constraint on sampling frequency and computation time compared with the Hilbert transform, which requires sampling at a much higher rate than f_r. In each channel, axial ranging was performed by recording of the amplitude of the corresponding demodulated interferometric signal:

$$g_i(t) = |g_i(t)|\exp\{-j[2\pi f_{s,i}t + \beta_i(t)]\}, \qquad (1)$$

where, for channel $i = 1, 2$, $|g_i(t)|$ is the amplitude reflectivity, $f_{s,i}$ is the Doppler frequency induced by flowing scatterers in the sample arm, and $\beta_i(t)$ is an

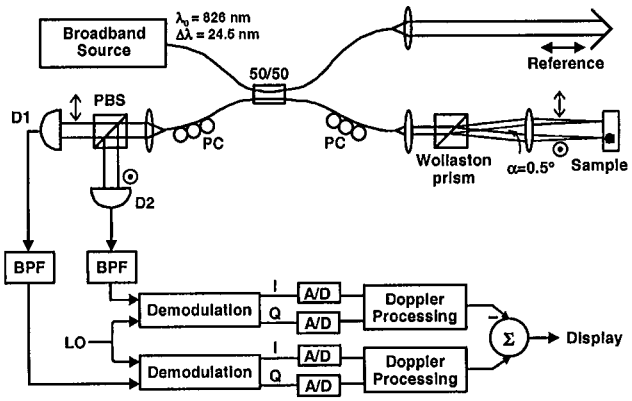

Fig. 1. Fiber-optic self-referenced DOCT Michelson interferometer with polarization diversity detection. Differential phase contrast between the two detected polarization channels was used to eliminate common-mode frequency noise in the interferometer. PCs, polarization-controlling paddles; PBS, polarizing beam splitter; D1, D2, SI photodetectors; BPFs, bandpass filters; LO, local oscillator; A/D's, analog–digital converters; I, Q, in-phase and quadrature signal components, respectively, after demodulation.

0146-9592/02/232085-03$15.00/0

additional term containing phase fluctuations. These fluctuations include but are not limited to mechanical vibrations, thermal drifts, phase noise in the electronic pathway (e.g., detectors, filters, lock-ins), nonlinearities in the reference-arm scan rate, and sample motion.

Several processing algorithms have been implemented for extracting the instantaneous (i.e., depth-dependent) sample-arm frequency $f_{s,i}$ from Eq. (1). Following the initial demonstrations of off-line numerical processing by time–frequency analysis[2] or the Hilbert transform,[3] real-time blood flow imaging was demonstrated *in vivo* by an autocorrelation algorithm implemented in hardware.[15,16] All these algorithms assumed that changes in $\beta(t)$ are negligible over the duration used to calculate f_s. Although this assumption is often valid, abrupt sample motion can cause artifacts in the measurement of f_s. Self-referenced DOCT uses the differential phase between two channels to eliminate common-mode fluctuations of $\beta(t)$. We performed Doppler processing by computing the autocorrelation of the complex demodulated data [Eq. (1)] from each polarization channel,

$$R_i(\tau) = |R_i(\tau)|\exp[-i\phi_i(\tau)] \equiv \langle g_i^*(t) g_i(t+\tau)\rangle, \quad (2)$$

for a single delay (lag) τ. In practice, the expected value (denoted by angle brackets) was implemented with a low-pass filter. The phase of the autocorrelation was expressed as

$$\phi_i(\tau) = 2\pi f_{s,i}\tau + \langle \beta_i(t+\tau) + \beta_i(\tau)\rangle. \quad (3)$$

Assuming that the second term (caused by phase fluctuations in the interferometer) was identical in both channels, the self-referenced differential phase of the autocorrelation reduced to

$$\phi_{\mathrm{SR}}(\tau) = \phi_2 - \phi_1 = 2\pi\tau(f_{s,2} - f_{s,1}) = 2\pi\tau\Delta f_s, \quad (4)$$

thus eliminating interferometer noise such as sample motion artifacts. The differential Doppler frequency observed between the two channels was therefore calculated as the differential phase of the autocorrelation divided by the lag τ of the autocorrelation, equal to the axial sampling increment τ_{PIXEL}.

The frequency precision is inversely related to the observation time $T = N\tau$, where $\tau = \tau_{\mathrm{PIXEL}}$ and N is the number of pixels over which the expected value is calculated. To increase velocity sensitivity, we implemented sequential scan processing.[8,16] Here Eq. (2) can be rewritten as

$$R_{i,m}(\tau) = \langle g_{i,m}^*(t) g_{i,m+1}(t)\rangle, \quad (5)$$

where the autocorrelation is computed across sequential scans m and $m+1$ and τ becomes the time between axial scans, τ_{SCAN}. Therefore, T becomes dependent on τ_{SCAN} rather than τ_{PIXEL}, resulting in a velocity sensitivity improvement by the ratio $\tau_{\mathrm{SCAN}}/\tau_{\mathrm{PIXEL}}$.

To verify the self-referenced DOCT algorithm, we performed imaging on a specular reflection from a mirror in the sample arm. Noise cancellation with subhertz sensitivity was demonstrated by manual dithering of the mirror during image acquisition to induce phase noise. Depth-resolved Doppler frequency profiles for $f_{s,1}$, $f_{s,2}$, and Δf_s calculated by sequential scan processing are shown in Fig. 2 for a single line scan. Arbitrary phase jumps and offsets in the individual channels were eliminated in the differential measurement. The standard deviation of the frequency noise was reduced from 3.5 to 0.11 Hz.

An intravenous fat emulsion (Liposyn, 0.8% solid) was chosen as a highly scattering sample. In an aqueous suspension, Brownian motion of the scattering particles leads to spectral broadening,[7] $\Omega = 16(\pi/\lambda)^2 D_T$, that may limit the Doppler frequency sensitivity. The average translational diffusion coefficient of Liposyn particles ($D_T = 1.1 \times 10^{-8}$ cm^2/s) resulted in spectral broadening of roughly 40 Hz, an order of magnitude greater than the sequential scan processing Nyquist frequency of $1/2\tau_{\mathrm{SCAN}} \sim 5$ Hz. Therefore, in the case of the scattering solution, we implemented axial processing [Eq. (2)] to increase the Nyquist frequency to $1/2\tau_{\mathrm{SCAN}} \sim 13$ kHz, well above the Brownian motion limit.

To demonstrate self-referenced velocimetry in a scattering medium, we induced interferometer phase noise by intentionally detuning the reference-arm galvanometer driver. Figure 3 displays DOCT images before and after differential phase correction. The horizontal lines in Fig. 3A are due to the variations in the reference-arm Doppler shift from its nominal value. Depth-resolved frequency profiles are shown in Fig. 3C. Although the Doppler shifts in each channel that result from the detuned reference scan varied over a large range ($\sigma = 1.74$ kHz), the differential measurement reduced these variations to 0.37 kHz. Next, self-referenced DOCT was demonstrated on a flow phantom consisting of a glass capillary tube (I.D. = 0.5 mm) mounted at ~70° with respect to the optical axis and immersed in Liposyn. A precision infusion syringe pump delivered the fluid into the phantom at 3.86 mL/h. The beam separation of 863 μm ensured that in a cross-sectional image of the capillary tube one beam remained in the nonflowing portion of the phantom while the other beam was focused in the tube. Therefore the flowing Liposyn

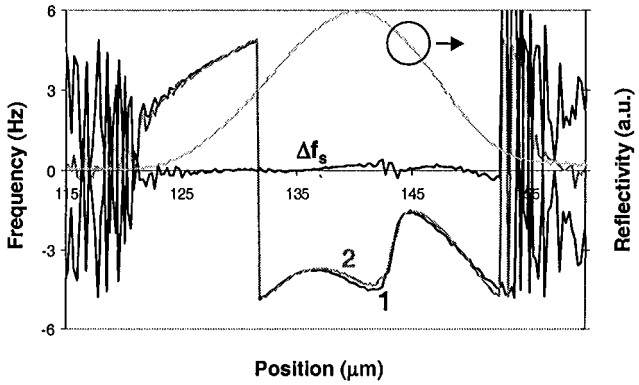

Fig. 2. Depth-resolved Doppler frequency profiles from a manually dithered mirror. The individual polarization channels demonstrate phase wrapping and fluctuations. Subtracting the two profiles results in a self-referenced profile with subhertz frequency noise. The standard deviation of the noise was reduced from 3.5 to 0.11 Hz.

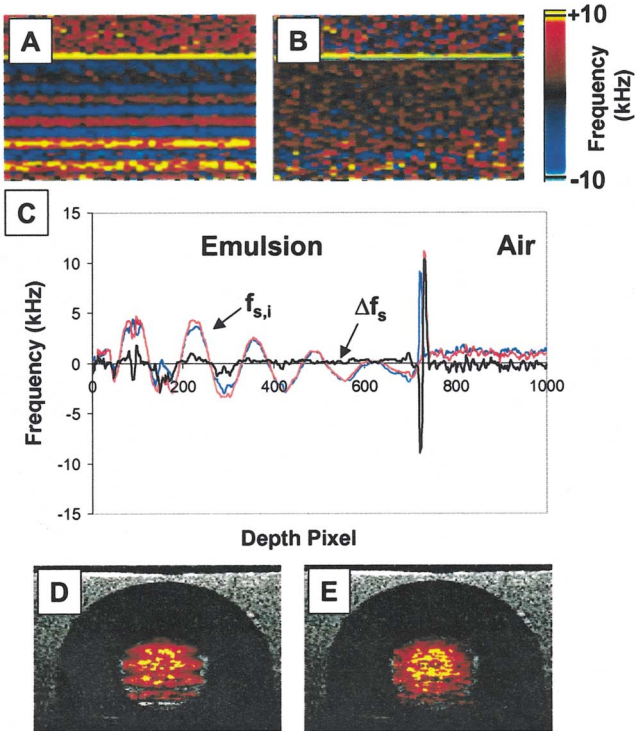

Fig. 3. A, Single-channel DOCT image of a stationary Liposyn phantom. The horizontal lines were caused by the depth-dependent variations of the reference from its nominal velocity, which we intentionally induced to simulate interferometer noise. B, Self-referenced DOCT image illustrates nearly complete cancellation of the reference-arm noise that is present in both channels. C, Average of 40 depth profiles from images A and B. Excluding the surface reflection artifact, frequency variations were reduced from $\sigma = 1.74$ kHz to $\sigma = 37$ kHz, comparable to a frequency precision[4] of 0.26 kHz with $N = 16$ and $1/\tau_{\text{pixel}} = 26$ kHz and assuming a Gaussian random noise process[4] with 40 samples. $f_{s,i}$, sample-arm Doppler frequency for channel $i = 1, 2$; Δf_s, differential Doppler shift. D, Cross-sectional DOCT of glass capillary tube with flowing Liposyn. E, Self-referenced DOCT image indicates that the flow information was encoded in the differential frequency component Δf_s, whereas the common-mode reference-arm noise was eliminated.

modulated only one of the beams, whereas both beams detected the common-mode noise induced by bulk motions of the flow phantom and the nonlinearities in the reference scan. Cross-sectional images of the phantom (Figs. 3D and 3E) demonstrate nearly complete elimination of the parasitic noise while maintaining the differential Doppler shift component induced by the flowing scatterers. Removing only the common-mode frequency component indicates that cross talk between the two polarization channels was not responsible for the correction. If cross talk is significant, both the signal and the noise become common mode ($\Delta f_s \sim 0$). Cross talk can be completely eliminated[10] with the introduction of a Lyot depolarizer in the source arm and a polarization-maintaining fiber coupler in the interferometer.

Self-referenced DOCT may become useful *in vivo*, where blood flow is measured in the presence of bulk motion artifacts. A smaller beam separation may be used *in vivo* since blood vessels of interest are typically smaller than the flow phantom used in the experiments. As the beam separation is reduced (i.e., $\lim \Delta x \rightarrow 0$) the differential velocity measured with self-referenced DOCT approaches the derivative of the flow profile. However, a large beam separation may be used to reference measurement of flow in a vessel to an avascular region of the tissue, mimicking the results reported in this Letter. In conclusion, we have presented a method of self-referenced Doppler velocimetry based on polarization diversity differential phase contrast OCT.

The authors gratefully acknowledge the help of A. Husain and M. A. Choma and fruitful discussions with C. Yang and A. M. Rollins. This study was supported by National Institutes of Health grant EY-13015. J. Izatt's e-mail address is jizatt@duke.edu.

References

1. D. Huang, E. A. Swanson, C. P. Lin, J. S. Schuman, W. G. Stinson, W. Chang, M. R. Hee, T. Flotte, K. Gregory, C. A. Puliafito, and J. G. Fujimoto, Science **254,** 1178 (1991).
2. J. A. Izatt, M. D. Kulkarni, S. Yazdanfar, J. K. Barton, and A. J. Welch, Opt. Lett. **22,** 1439 (1997).
3. Y. Zhao, Z. P. Chen, C. Saxer, S. Xiang, J. F. de Boer, and J. S. Nelson, Opt. Lett. **25,** 114 (2000).
4. M. D. Kulkarni, T. G. van Leeuwen, S. Yazdanfar, and J. A. Izatt, Opt. Lett. **23,** 1057 (1998).
5. S. Yazdanfar, A. M. Rollins, and J. A. Izatt, Opt. Lett. **25,** 1448 (2000).
6. A. V. Zvyagin, J. B. FitzGerald, K. K. M. B. D. Silva, and D. D. Sampson, Opt. Lett. **25,** 1645 (2000).
7. D. A. Boas, K. K. Bizheva, and A. M. Siegel, Opt. Lett. **23,** 319 (1998).
8. S. Yazdanfar, A. M. Rollins, and J. A. Izatt, Proc. SPIE **4251,** 156 (2001).
9. C. K. Hitzenberger and A. F. Fercher, Opt. Lett. **24,** 622 (1999).
10. D. P. Davé and T. E. Milner, Opt. Lett. **25,** 227 (2000).
11. C. Yang, A. Wax, I. Georgakoudi, E. B. Hanlon, K. Badizadegan, R. R. Dasari, and M. S. Feld, Opt. Lett. **25,** 1526 (2000).
12. C. C. Williams and H. K. Wickramasinghe, J. Appl. Phys. **60,** 1900 (1986).
13. C. Yang, A. Wax, M. S. Hahn, K. Badizadegan, R. R. Dasari, and M. S. Feld, Opt. Lett. **26,** 1271 (2001).
14. C. Yang, A. Wax, R. R. Dasari, and M. S. Feld, Opt. Lett. **27,** 77 (2002).
15. A. M. Rollins, S. Yazdanfar, J. K. Barton, and J. A. Izatt, J. Biomed. Opt. **7,** 123 (2002).
16. V. Westphal, S. Yazdanfar, A. M. Rollins, and J. A. Izatt, Opt. Lett. **27,** 34 (2002).